Electrochemical and Structural Investigation of the Interactions between Naphthalene Diimides and Metal Cations

SUPPORTING INFORMATION

Benjamin R. Reiner, Bruce M. Foxman, and Casey R. Wade*

Department of Chemistry, Brandeis University, 415 South Street, Waltham, Massachusetts 02453.

Contents ***Pages***

Calculation of β.[S1]

The formation constants for $NDIM_p^{(-1+np)}$ and $NDIM_q^{(-2+nq)}$ can be expressed with equations (1a) and (1b), respectively. M^{n+} represents the metal cations Li^+ or Mg^{2+} and p and q represent the stoichiometry of cation complexation.

$$\beta_{ox} \quad NDI^{\cdot -} + pM^{n+} \rightleftharpoons NDIM_p^{(-1+np)} \qquad (1a)$$

$$\beta_{red} \quad NDI^{-2} + qM^{n+} \rightleftharpoons NDIM_q^{(-2+nq)} \qquad (1b)$$

The expression describing the relationship of these equilibria to the Nernst equation is shown by equation (2) where: ΔE_{pc} represents the difference between the peak cathodic potential in the absence and presence of metal cation additive, z is number of electrons transferred, and the constant, 0.05916, assumes STP.

$$\Delta E_{pc} = \frac{0.05916}{z} \log\left(\frac{1+\beta_{red}[M^{n+}]^q}{1+\beta_{ox}[M^{n+}]^p}\right) \qquad (2)$$

The CV titration data shows negligible shifts in the $NDI^{0/\cdot -}$ redox couple, but large shifts in the $NDI^{\cdot -/2-}$ redox couple. These observations suggest that while the NDI dianion interacts strongly with charge dense cations, the NDI radical anion does not. Therefore $\beta_{red} >> 1$ and $\beta_{ox} << 1$ and after rearrangement equation (2) reduces to equation (3). Note in the manuscript, in equation (1), the term $(q-p)$ has been reduced to q for simplicity.

$$\Delta E_{pc} = \frac{0.05916}{z} \log(\beta_{red}) - (q-p)\frac{0.05916}{z} \log([M^{n+}]) \qquad (3)$$

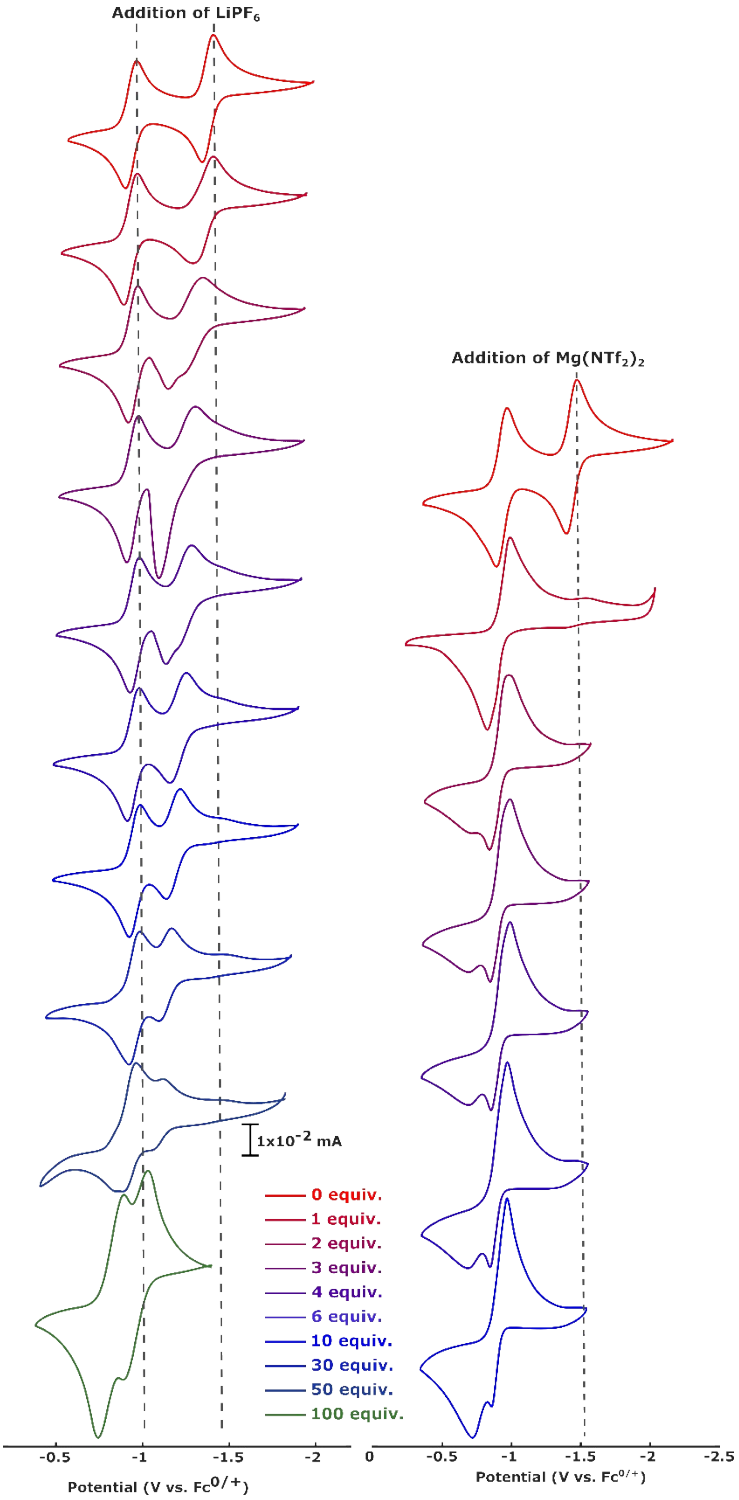

Figure S1. Cyclic voltammograms collected in MeCN with 0 – 100 equivalents of $LiPF_6$ (left) or $Mg(NTf_2)_2$ (right) at 100 mV/s, 1 mM $Dipp_2NDI$ in 0.1 M $TBAPF_6$ supporting electrolyte, glassy carbon working electrode, platinum wire counter electrode**,** and a Ag/AgCl wire pseudoreference, with ferrocene (Fc) added as an internal reference.

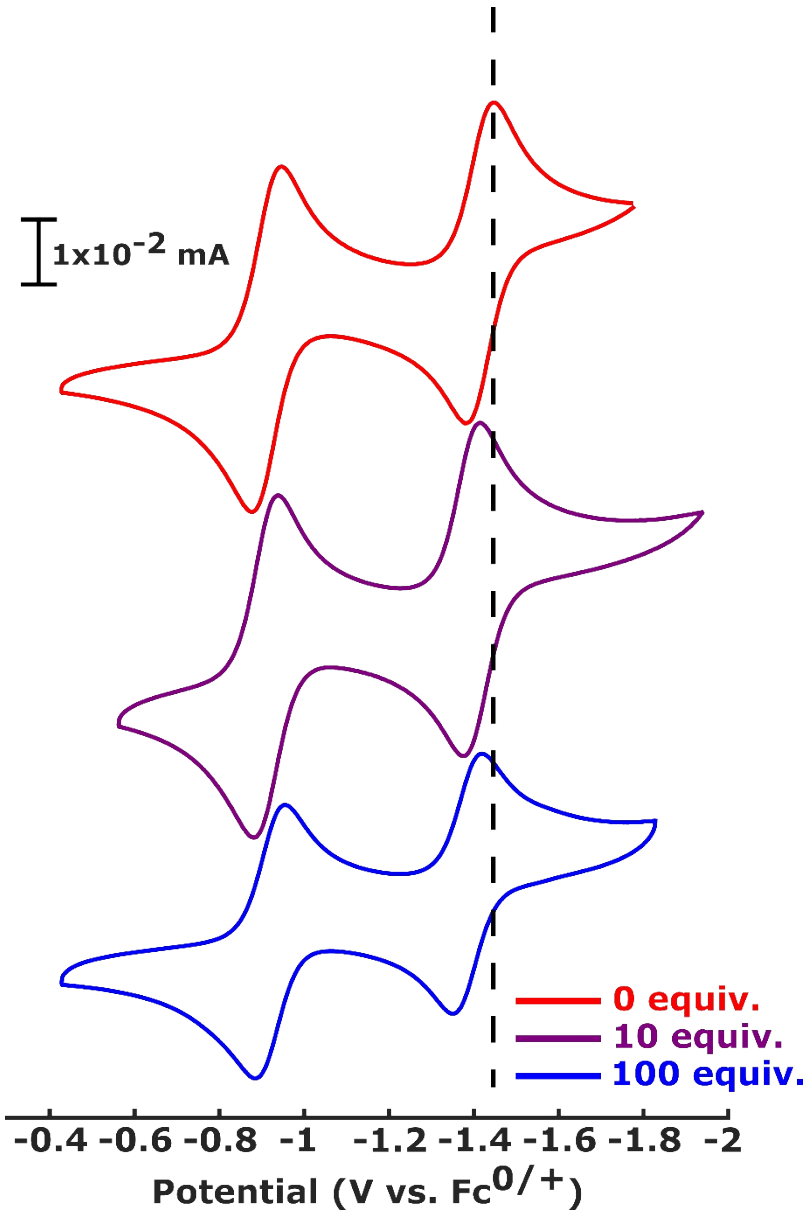

Figure S2. Cyclic voltammograms collected in MeCN with 0 – 100 equivalents of NaOTf at 100 mV/s, 1 mM $Dipp_2NDI$ in 0.1 M $TBAPF_6$ supporting electrolyte, glassy carbon working electrode, platinum wire counter electrode**,** and a Ag/AgCl wire pseudoreference, with ferrocene (Fc) added as an internal reference.

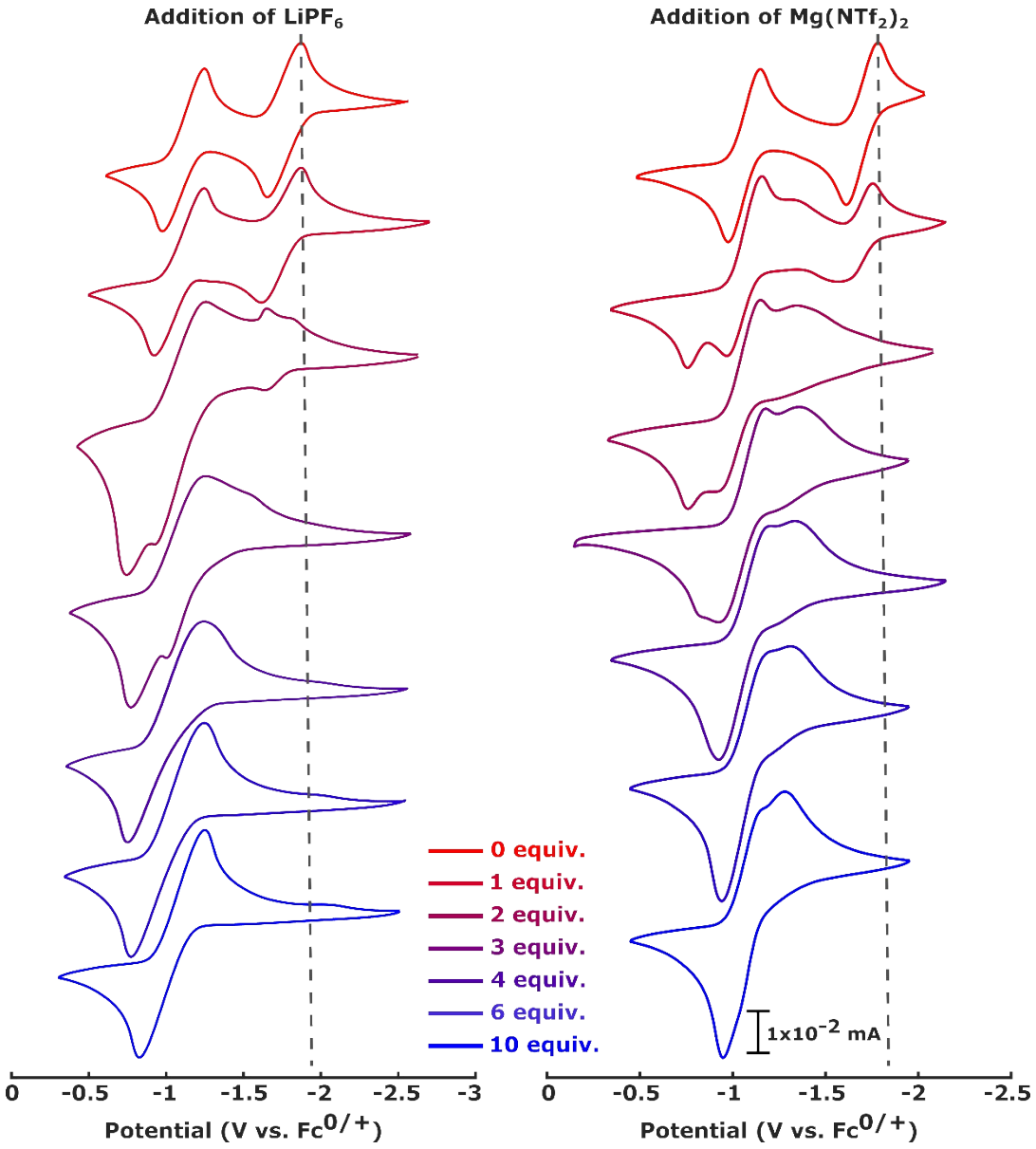

Figure S3. Cyclic voltammograms collected in THF with 0 – 10 equivalents of $LiPF_6$ (left) or $Mg(NTf_2)_2$ (right) at 100 mV/s, 1 mM $Dipp_2NDI$ in 0.1 M $TBAPF_6$ supporting electrolyte, glassy carbon working electrode, platinum wire counter electrode**,** and a Ag/AgCl wire pseudoreference, with ferrocene (Fc) added as an internal reference.

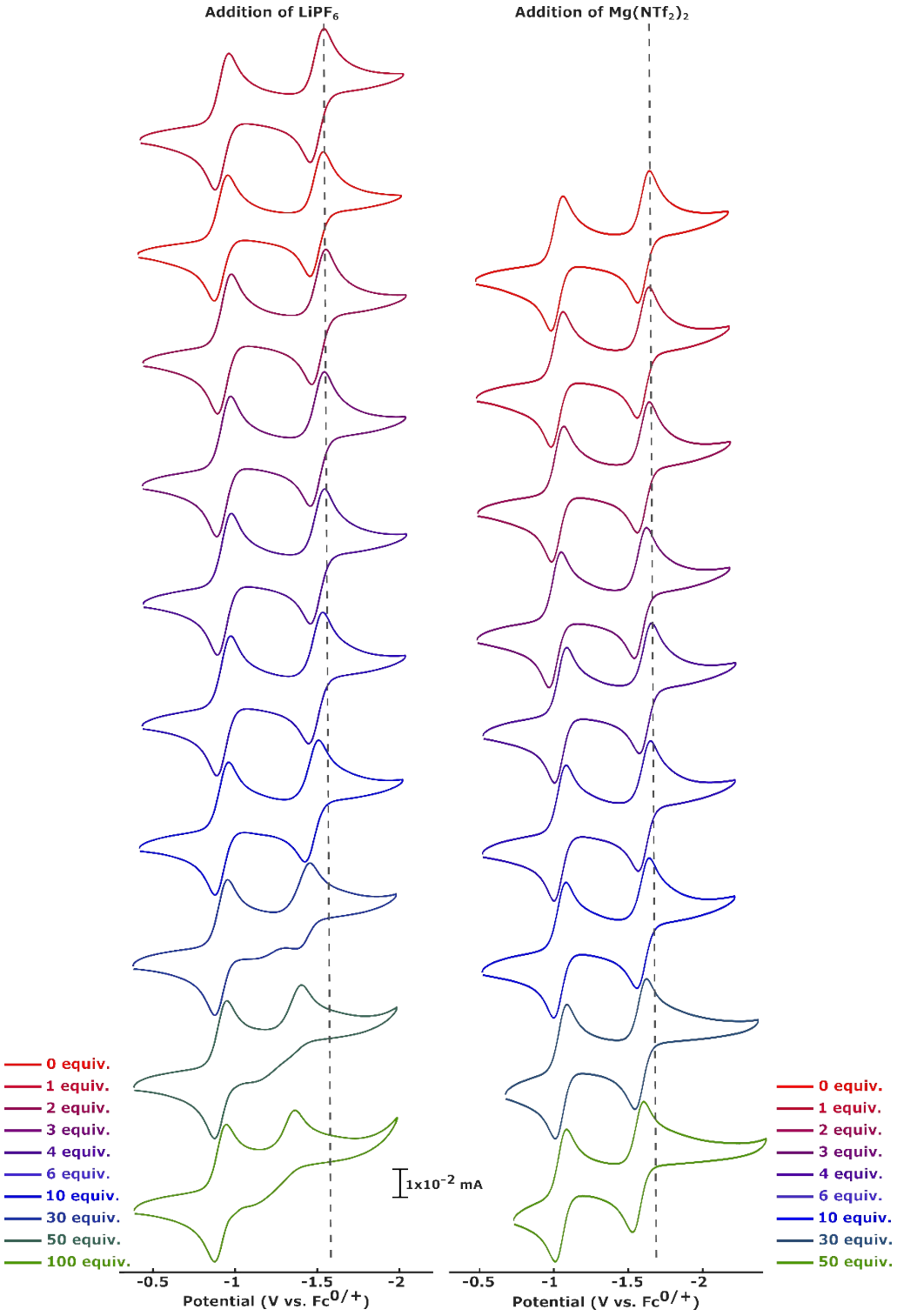

Figure S4. Cyclic voltammograms collected in DMF with 0 – 100 equivalents of $LiPF_6$ (left) or 0 – 50 equivalents of $Mg(NTf_2)_2$ (right) at 100 mV/s, 1 mM $Dipp_2NDI$ in 0.1 M $TBAPF_6$ supporting electrolyte, glassy carbon working electrode, platinum wire counter electrode**,** and a Ag/AgCl wire pseudoreference, with ferrocene (Fc) added as an internal reference.

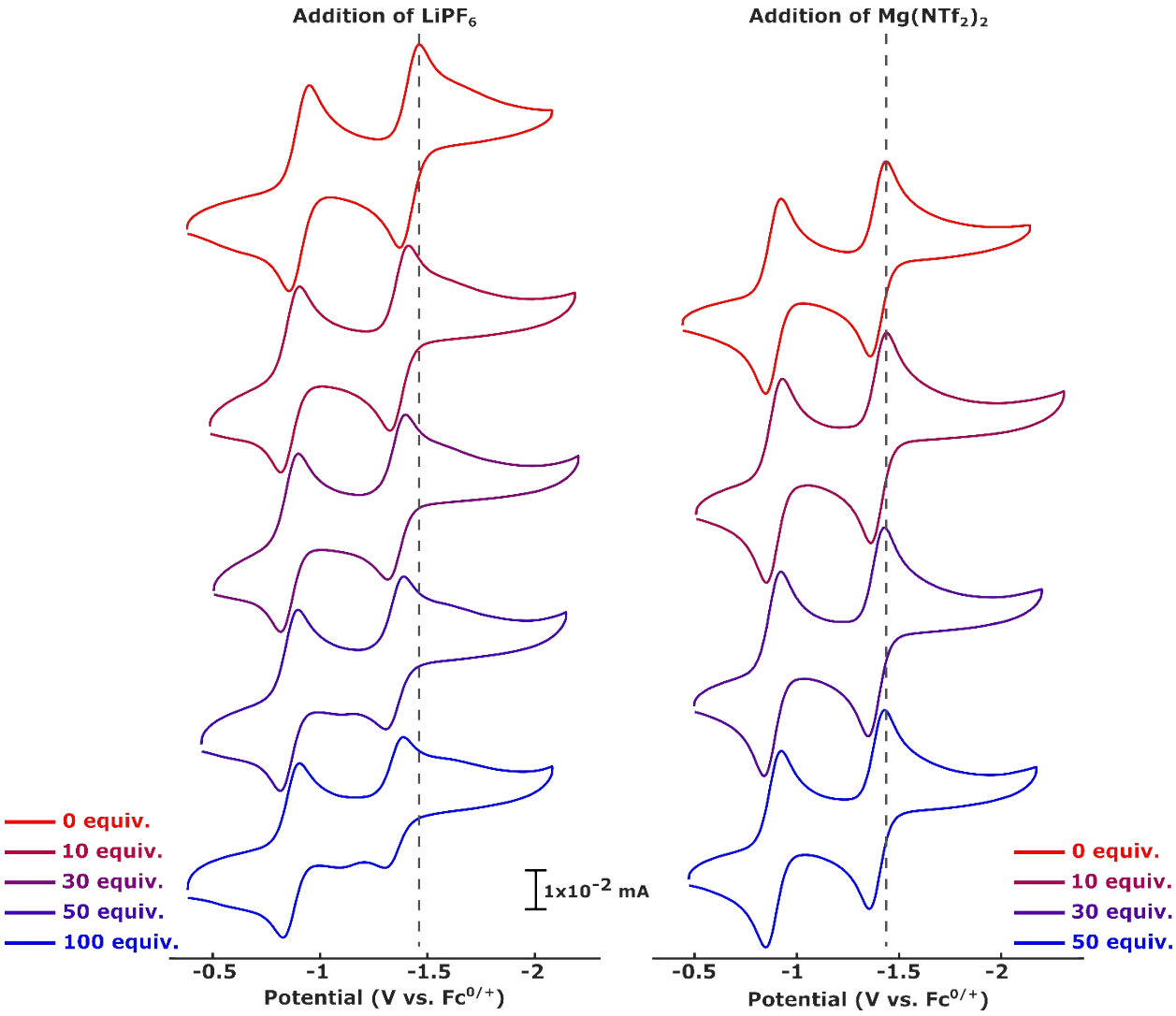

Figure S5. Cyclic voltammograms collected in DMSO with 0 – 100 equivalents of $LiPF_6$ (left) or 0 – 50 equivalents of $Mg(NTf_2)_2$ (right) at 100 mV/s, 1 mM $Dipp_2NDI$ in 0.1 M $TBAPF_6$ supporting electrolyte, glassy carbon working electrode, platinum wire counter electrode**,** and a Ag/AgCl wire pseudoreference with ferrocene (Fc) added as an internal reference.

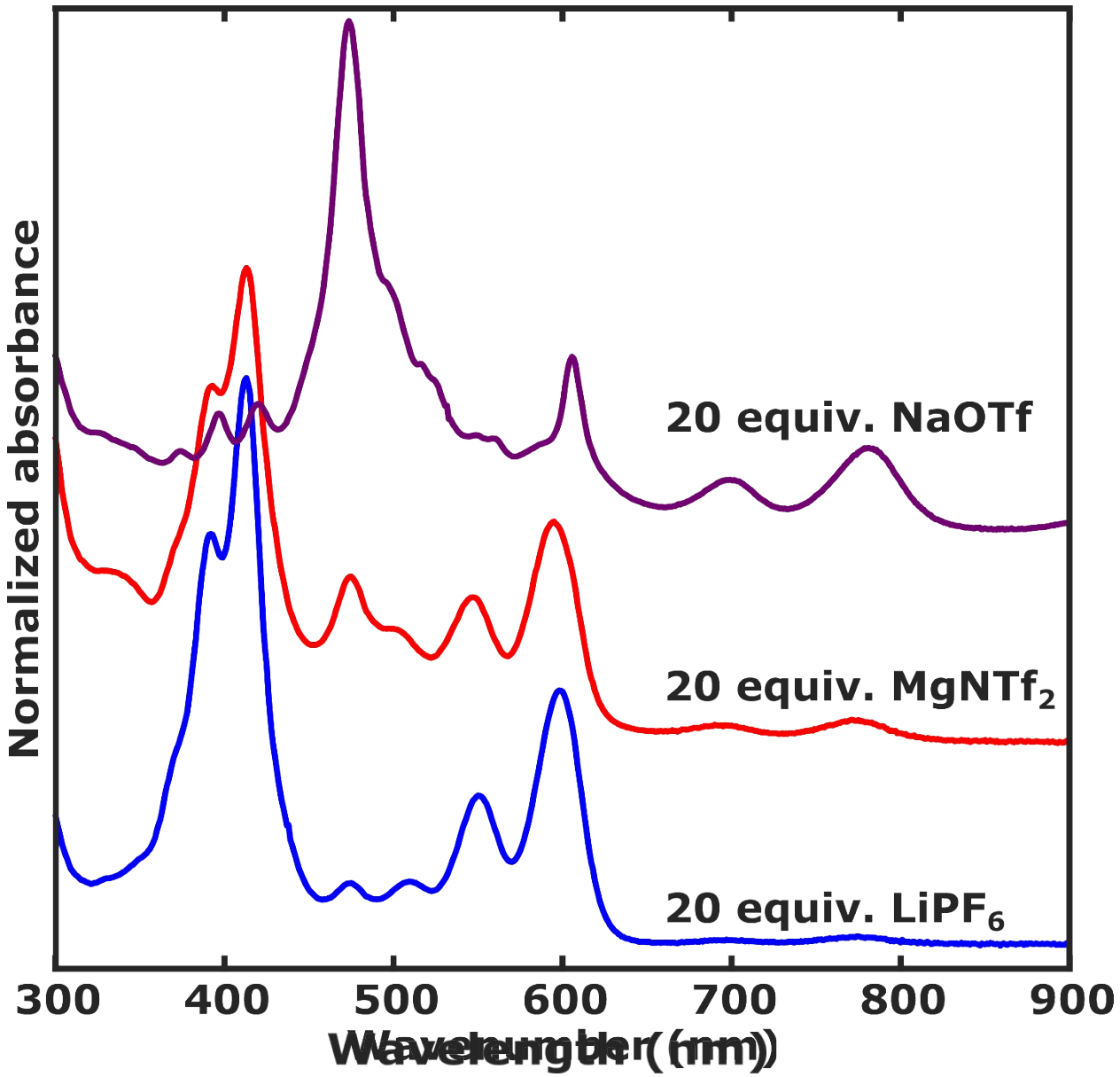

Figure S6. UV-vis spectra after UV irradiation (365 nm) of a solution of $Dipp_2NDI$ (8.9 μM), additive (180 μM), and Et_3N (0.17 M) in THF for 10 minutes.

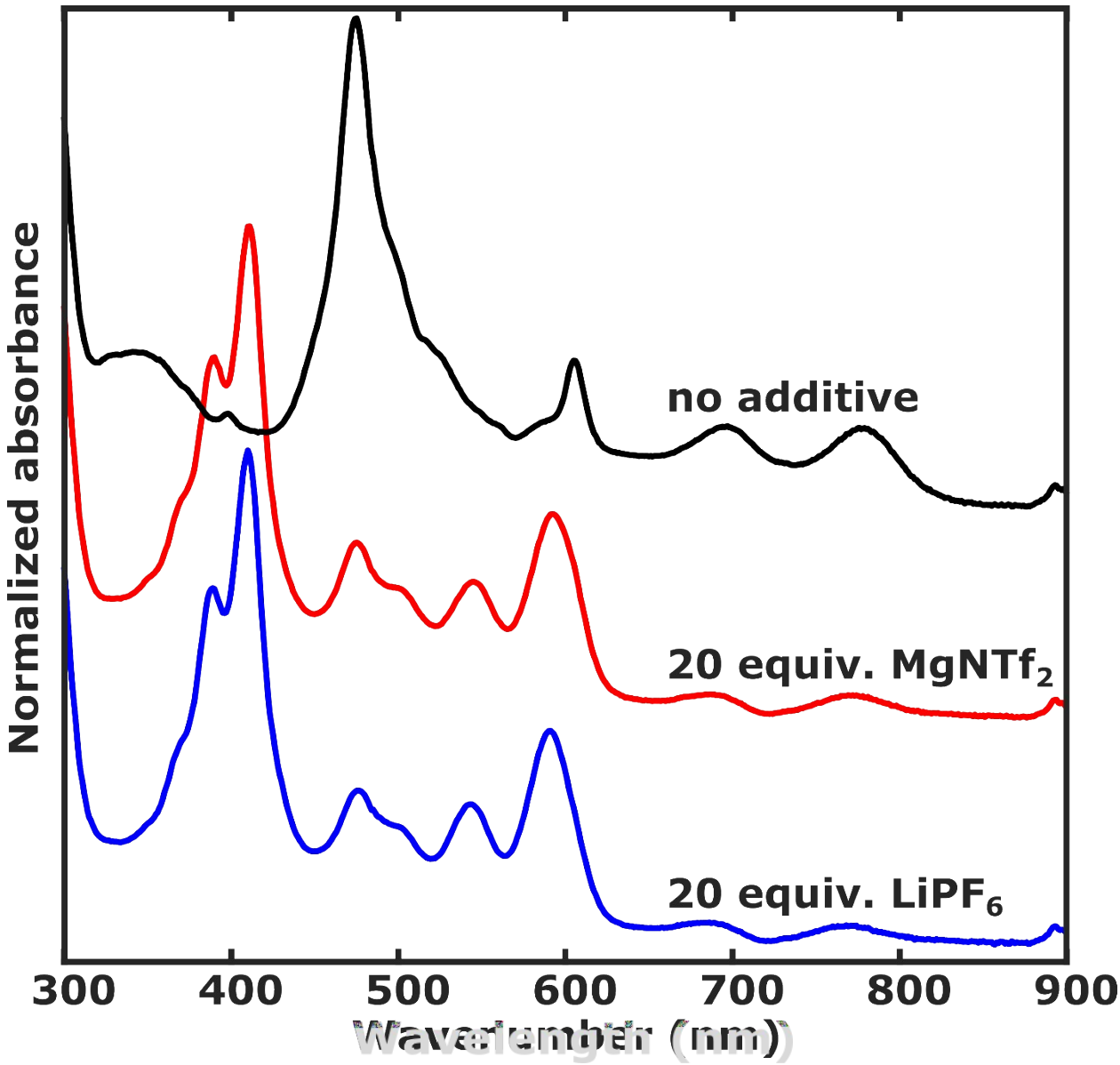

Figure S7. UV-vis spectra after UV irradiation (365 nm) of a solution of $Dipp_2NDI$ (8.9 μM), additive (180 μM), and Et_3N (0.17 M) in MeCN for 10 minutes.

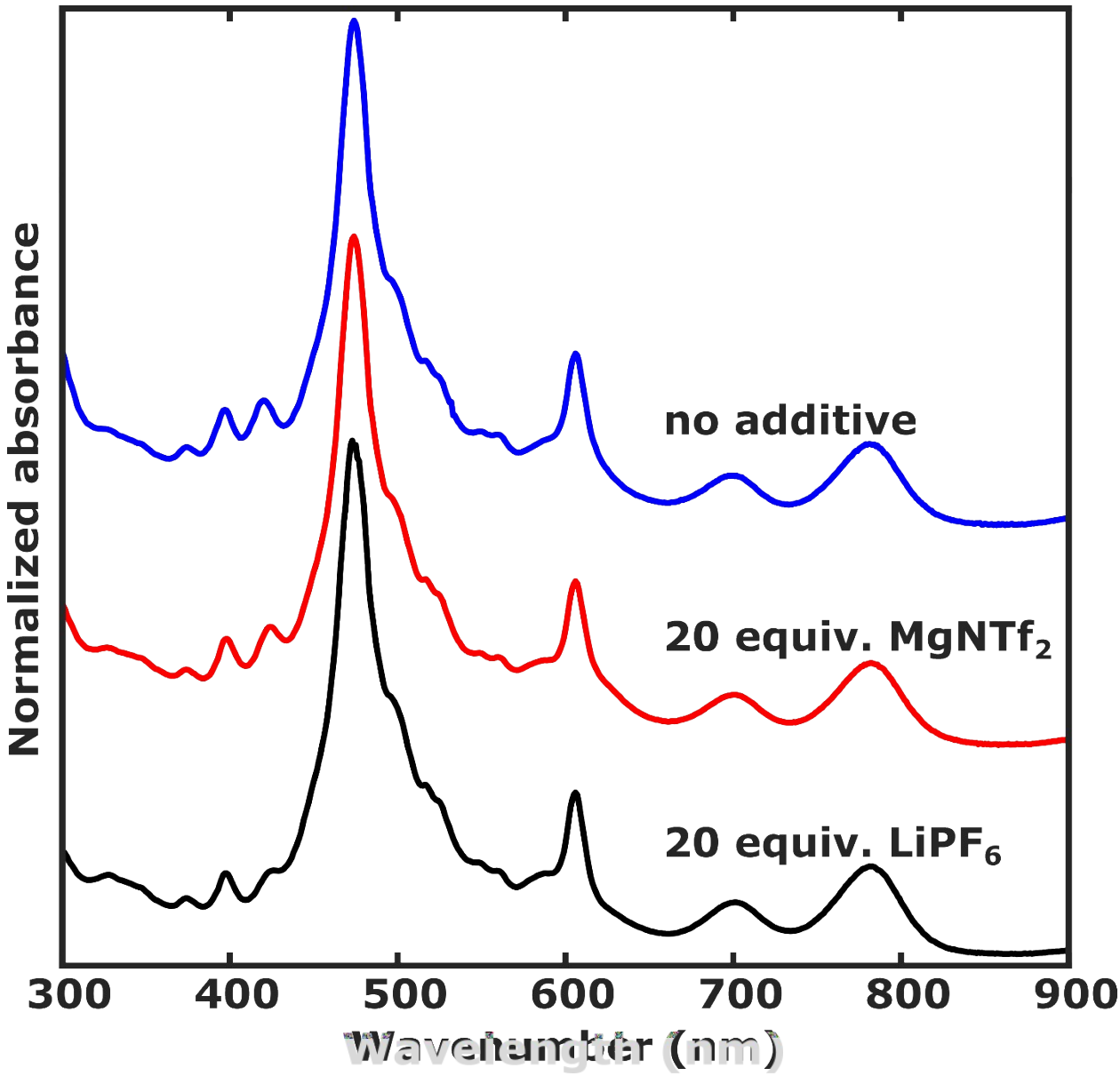

Figure S8. UV-vis spectra a after UV irradiation (365 nm) of a solution of $Dipp_2NDI$ (8.9 μM), additive (180 μM), and Et_3N (0.17 M) in DMF for 10 minutes.

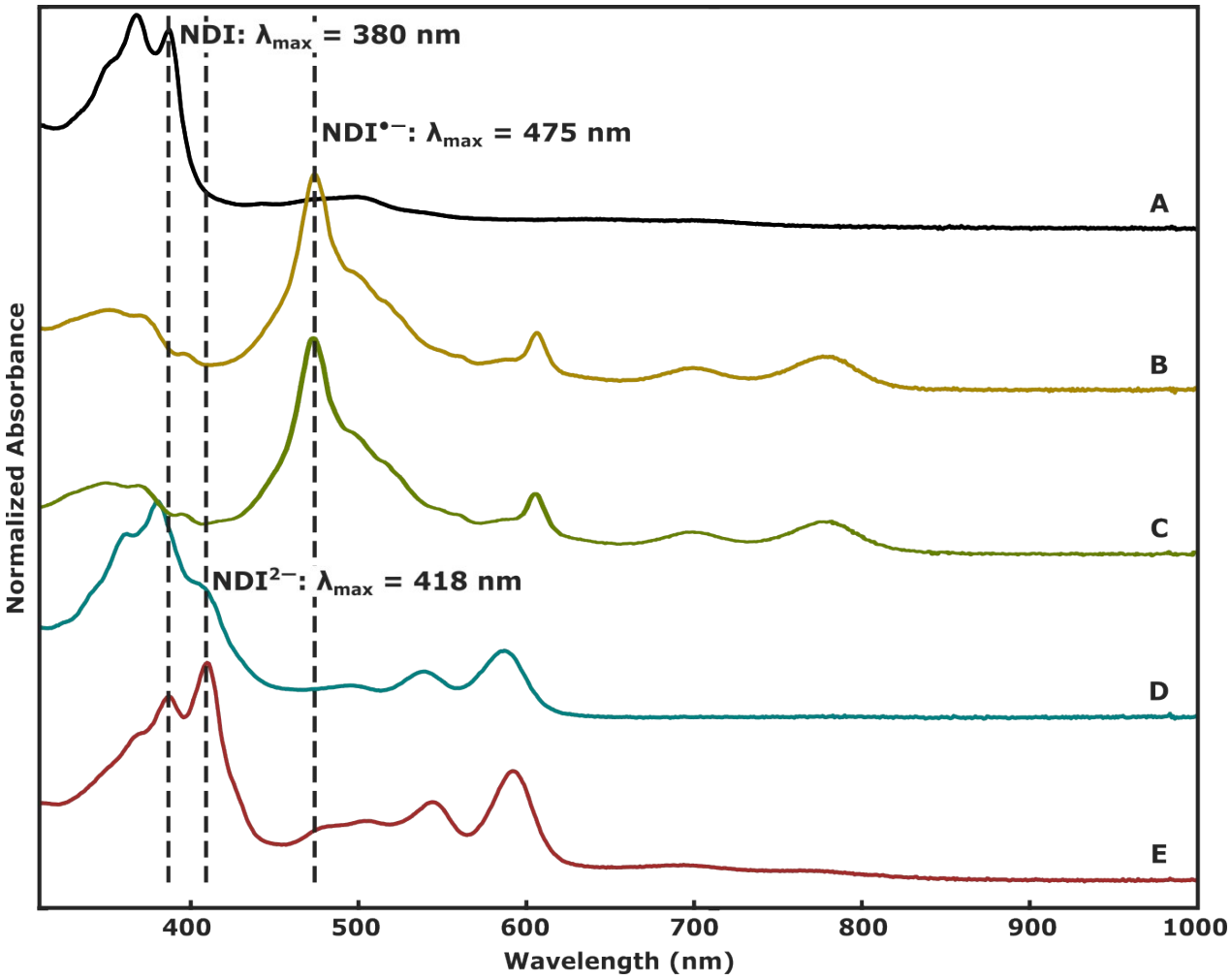

Figure S9. (a) UV-vis spectrum of a solution of $Dipp_2NDI$ (20 μM) in THF; **(b)** UV-vis spectrum of $[Dipp_2NDI]^{\cdot-}$ generated *in situ* by addition of NaHDMS (100 μM); UV-vis spectra of *in situ* generated $[Dipp_2NDI]^{\cdot-}$ in the presence of NaOTf (200 μM) **(c)**, $LiPF_6$ (200 μM) **(d)**, and $MgNTf_2$ (200 μM) **(e)**.

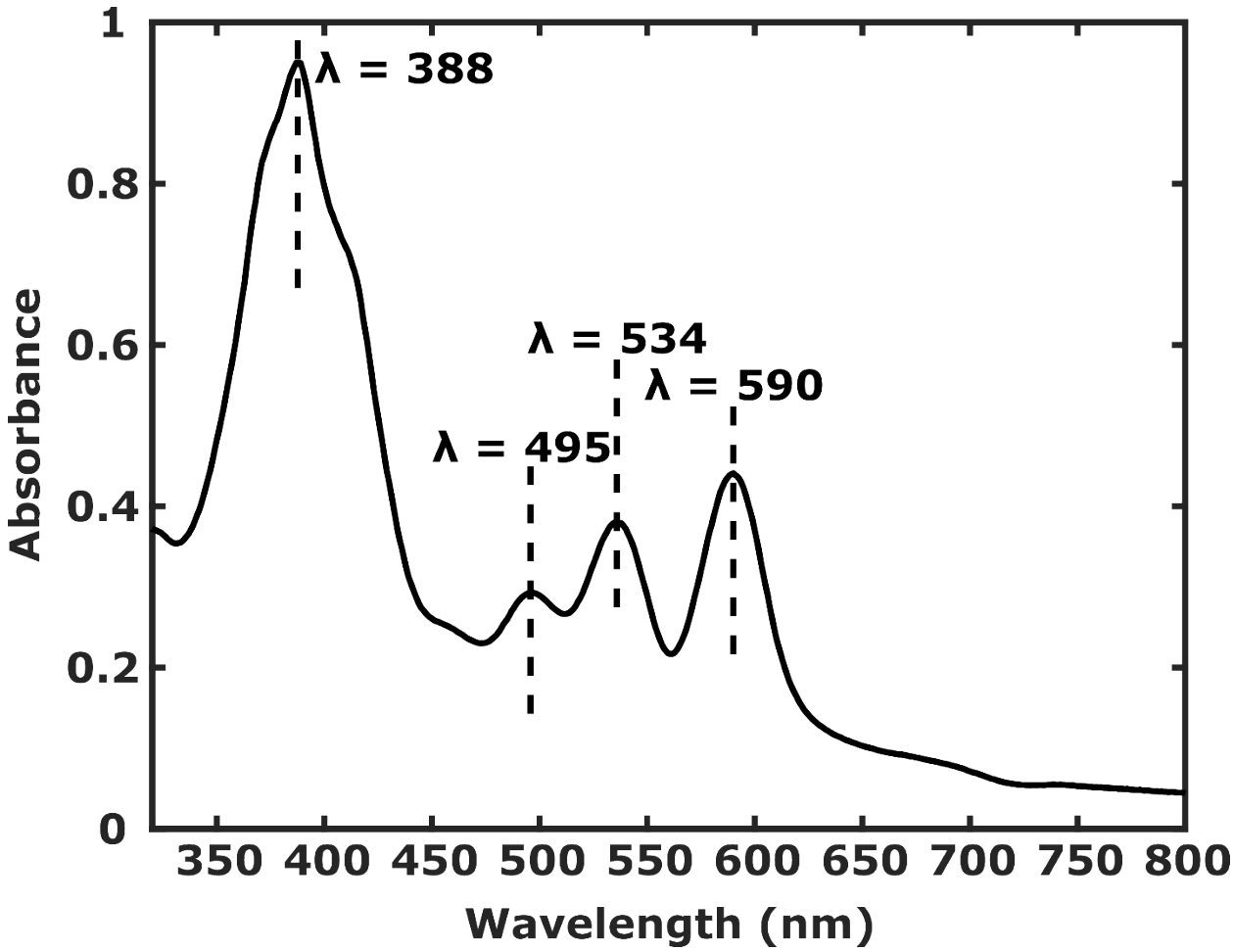

Figure S10. UV-Vis spectrum of **1** in THF.

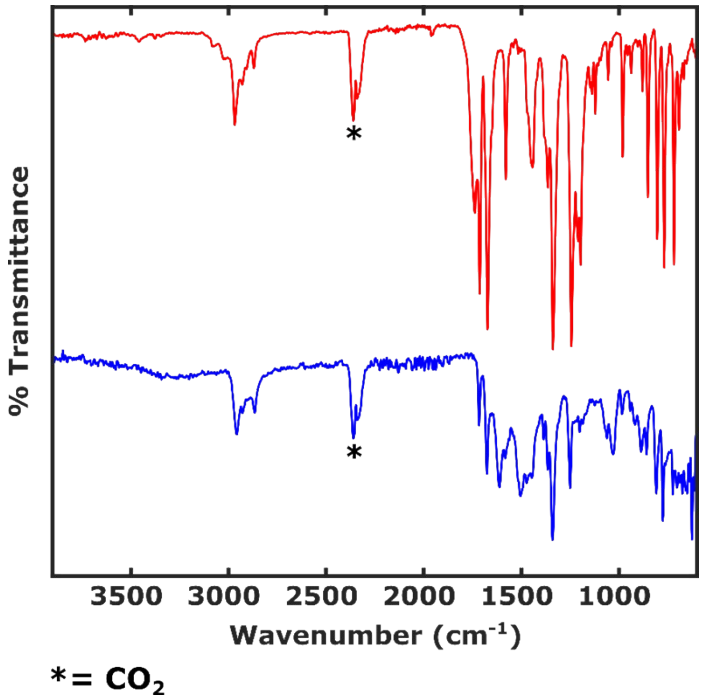

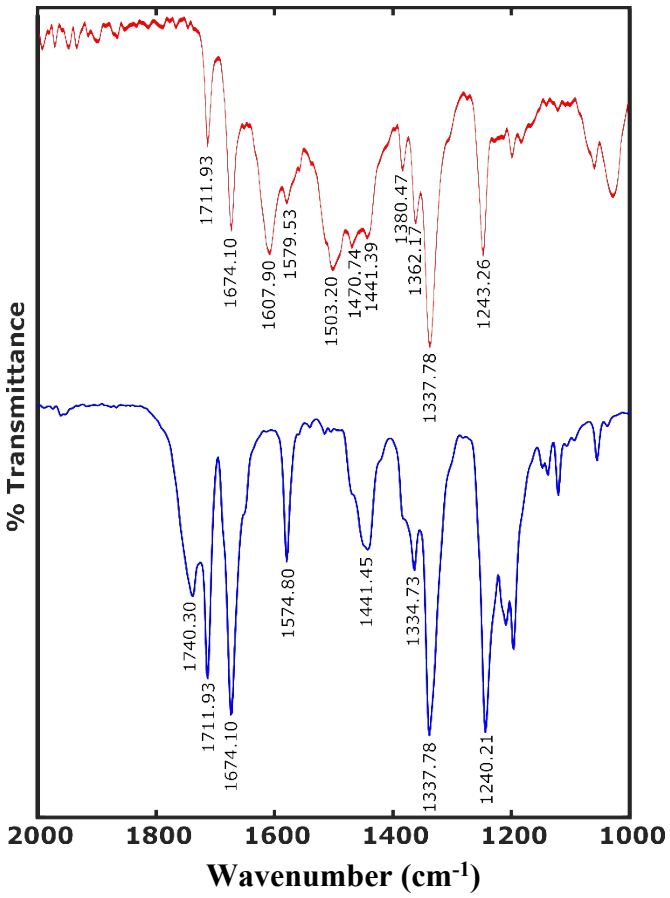

Figure S11. ATR-IR full spectra (top) and zoom (bottom) of **1** (red) and $Dipp_2NDI$ (blue).

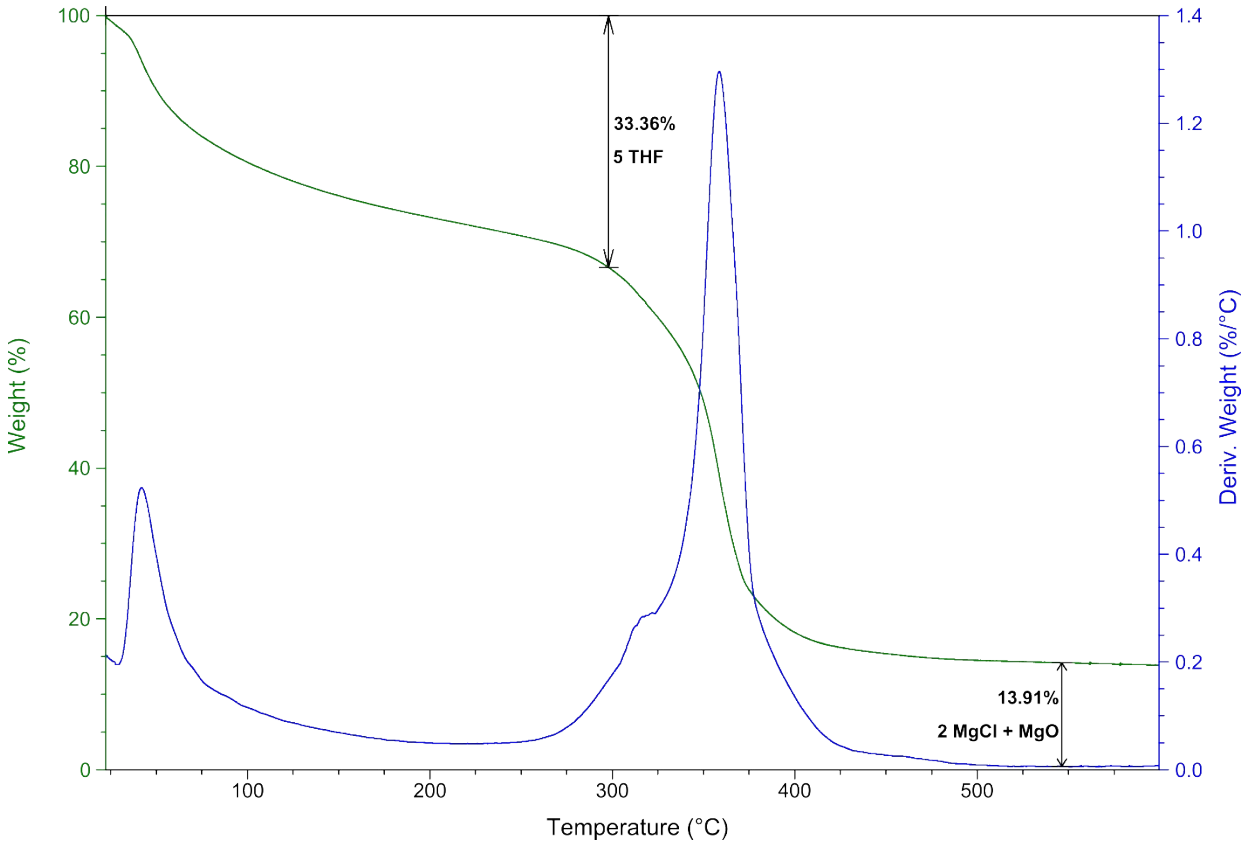

Figure S12. TGA data for **1** measured using a ramp rate of 2 °C/min

Reaction of 1 with MeOH. An NMR tube was charged with **1** (10 mg, 0.005 mmol). The dry powder was treated with MeOH (0.5 mL) which immeadiately afforded a green solution which turned to a pale yellow with concomitant precipitation of white crystalline material. The solution was spiked with $CDCl_3$ (0.1 mL) and mixed thoroughly to afford a homogenous solution. The reaction was analyzed by ^1H NMR which showed quanititative oxidation of **1** to the neutral parent $Dipp_2NDI$.

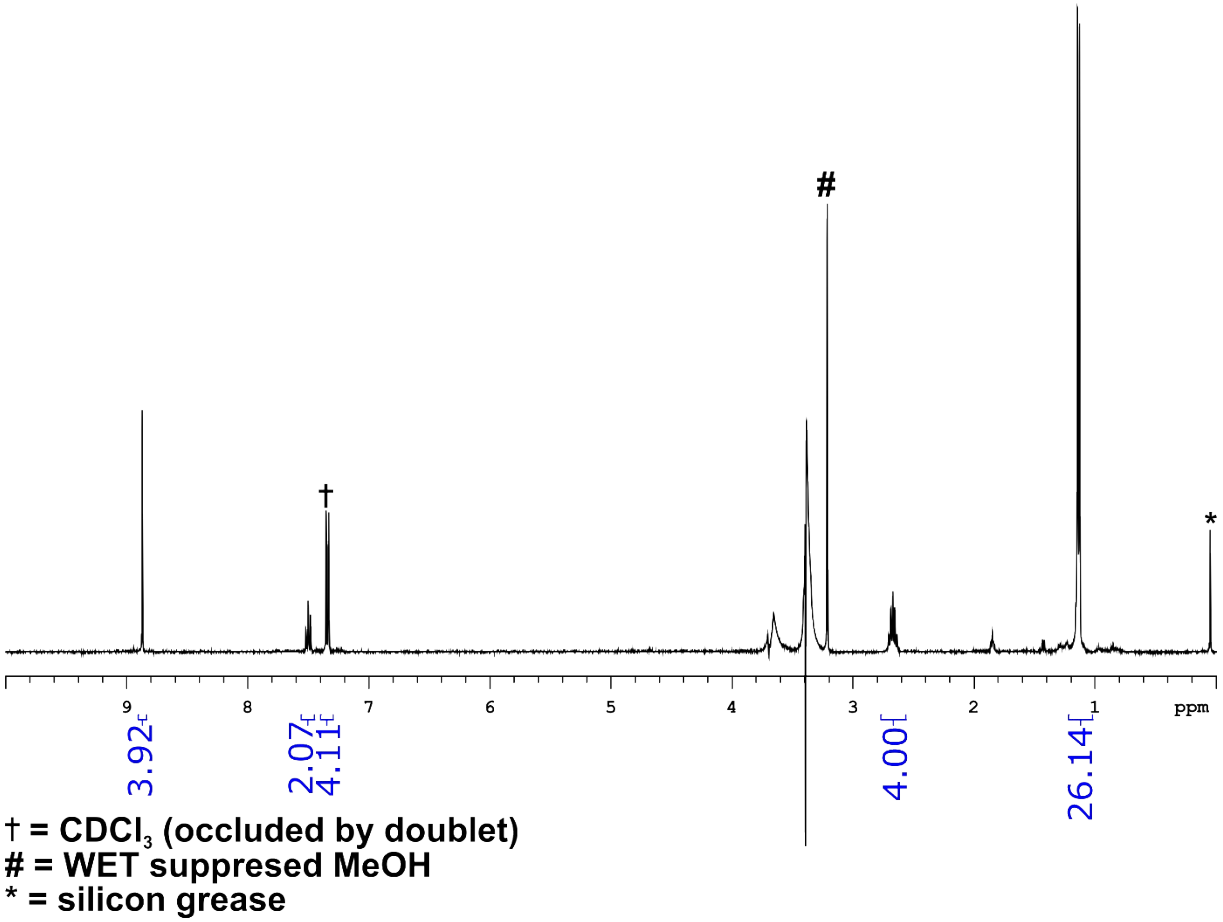

Figure S13. ^1H NMR spectrum of **1** treated with MeOH and spiked with $CDCl_3$.

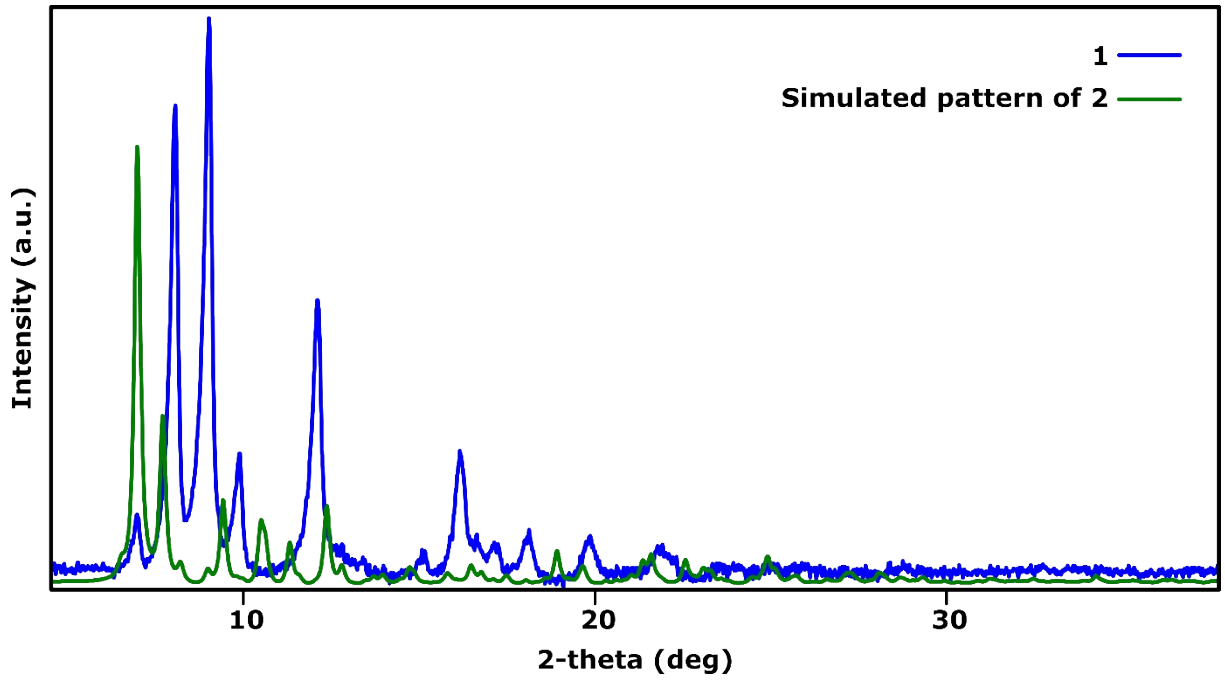

Figure S14. Overlay of the experimental powder X-ray diffraction (PXRD) pattern of **1** (blue) with the pattern simulated from the single crystal X-ray structure of **2** (green). Data was collected with Cu Kα radiation.

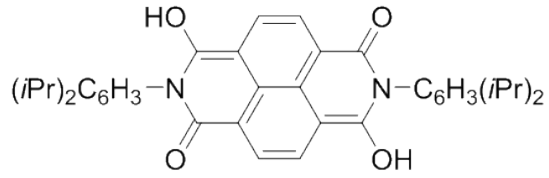

anti

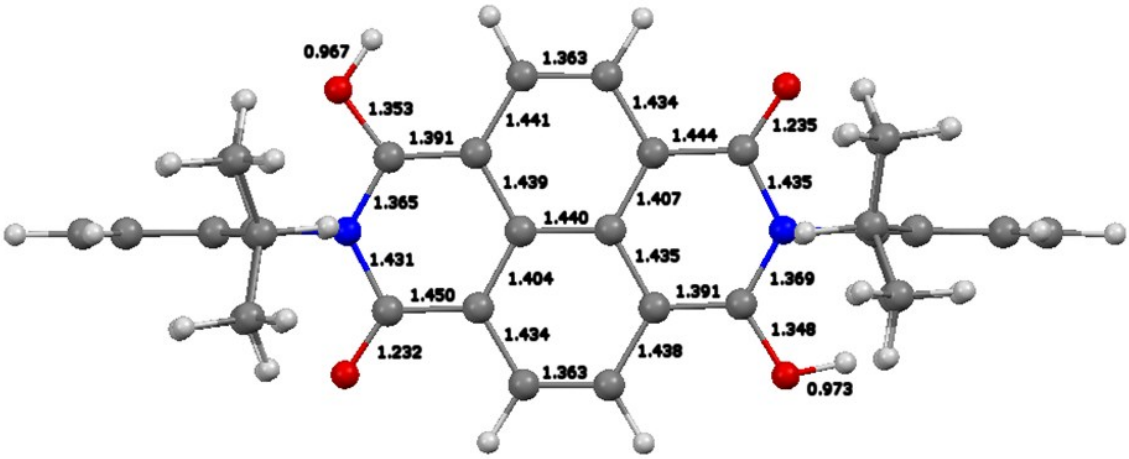

Single Point Energy: -1882. 73297 Ha

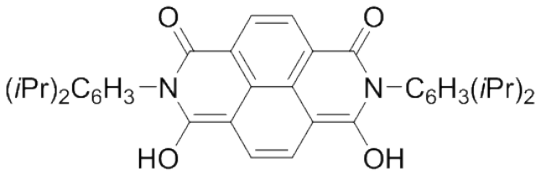

syn

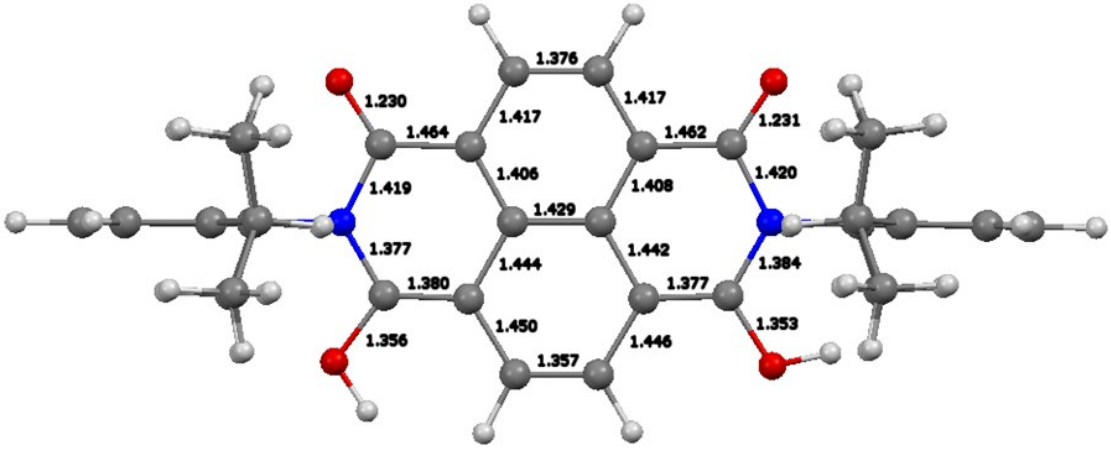

Single Point Energy: -1882.73832 Ha

Figure S15. DFT optimized structures and single point energies of *syn* and *anti* H_2[$Dipp_2$NDI].

Table S1. Crystallographic Data and Refinement Parameters for **2.**

chemical formula	$C_{100}H_{124}Mg_2N_4O_{14}$
fw	1654.72
T (K)	120
λ (Å)	0.71073
a (Å)	21.5029(15)
b (Å)	19.1115(14)
c (Å)	27.069(2)
α (deg)	90
β (deg)	90
γ (deg)	90
V (Å^3)	11124.1(14)
space group	*P*bca
Z, Z'	4, ½
D_{calcd} (g/cm^3)	0.99[b]
μ (cm^{-1})	0.075
R1 (I > 2σ (I))[a]	0.0892
wR2 (all data)[a]	0.2899

[a] $R1 = \sum |F_0| - |F_c| / \Sigma |F_0|$, $wR2 = \sum \left[w\left(F_o^2 - F_c^2\right)^2 \right] / \sum \left[w\left(F_o^2\right)^2 \right]$

[b] Does not include squeezed solvent

Details of X-Ray data collection, solution, and refinement for 2. All operations were performed on a Bruker-Nonius Kappa Apex2 diffractometer, using graphite-monochromated MoKα radiation. All diffractometer manipulations, including data collection, integration, scaling, and absorption corrections were carried out using the Bruker Apex2 software.[S2] Preliminary cell constants were obtained from three sets of 12 frames. Data collection was carried out at 120K, using a frame time of 120 sec and a detector distance of 60 mm. The optimized strategy used for data collection consisted of one phi and one omega scan set, with 0.5° steps in phi or omega; completeness was 99.9%. A total of 771 frames were collected. Final cell constants were obtained from the xyz centroids of 5037 reflections after integration.

From the systematic absences, the observed metric constants and intensity statistics, space group *Pbca* was chosen initially; subsequent solution and refinement confirmed the correctness of this choice. The structure was solved using *SIR-92*,[S3] and refined (full-matrix-least squares) using the Oxford University *Crystals for Windows* program.[S4] The asymmetric unit contains one-half molecule of the complex as well as (likely) two highly disordered THF solvate molecules, modeled using the SQUEEZE procedure (see below) (for the complex, $Z = 4$; $Z' = ½$). All ordered non-hydrogen atoms were refined using anisotropic displacement parameters. After location of H atoms on electron-density difference maps, the H atoms were initially refined with soft restraints on the bond lengths and angles to regularize their geometry (C---H in the range 0.93--0.98 Å and U_{iso} (H) in the range 1.2-1.5 times U_{eq} of the parent atom), after which the positions were refined with riding constraints.[S5] During the structure solution, electron density difference maps revealed that there were highly disordered solvate molecules, which could not be successfully modeled. Thus, from observations and reaction history, the remaining disordered solvate was assigned as THF in a volume of 2907.5 Å^3 per unit cell (26.1%). It appeared that the cavity area contained about 16 solvate molecules, located near the centers of symmetry at (½,0,0); (0,0,½); (½,½,½); (0,½,0), as shown in the *bc* projection below.[S6] Modeling with or without restraints was unsuccessful, as was step by step acquisition of peaks using successive electron density difference maps. Thus, the structure factors were modified using the PLATON SQUEEZE[S7] technique, in order to produce a "solvate-free" structure factor set. PLATON reported a total electron density of 712 e$^-$ per unit cell, likely representing about two THF molecules in the asymmetric unit (16 per unit cell would be 640 e-). Use of the SQUEEZE technique resulted in a decrease of *ca.* 6.3 % in *R*. Disorder in the THF molecules bound to Mg, as well as in the NDI dianion ligand bound to Mg, was partially resolved; occupancies of the major and minor components were constrained to sum to 1.0. For the bound THF ligands: [ligand 1: C(2,3) major / (C102,103) minor, occupancies: 0.587/0.413(18)]; [ligand 2: C106,107 major / C(6,7) minor, occupancies: 0.55/0.45(2)]; [ligand 3: C(11,12) major / (C111,112) minor, occupancies: 0.61/0.39(2)]. For the NDI dianion ligand bound to Mg: [O(5,6) + C(26-30, 37) major / O(105,106) + C(126-130, 137) minor, occupancies: 0.578/0.422(7)]. The final least-squares refinement converged to $R_1 = 0.0892$ ($I > 2\sigma(I)$, 4323 data) and $wR_2 = 0.2899$ (F^2, 8241 data, 531 parameters). The final CIF is available as supporting material.

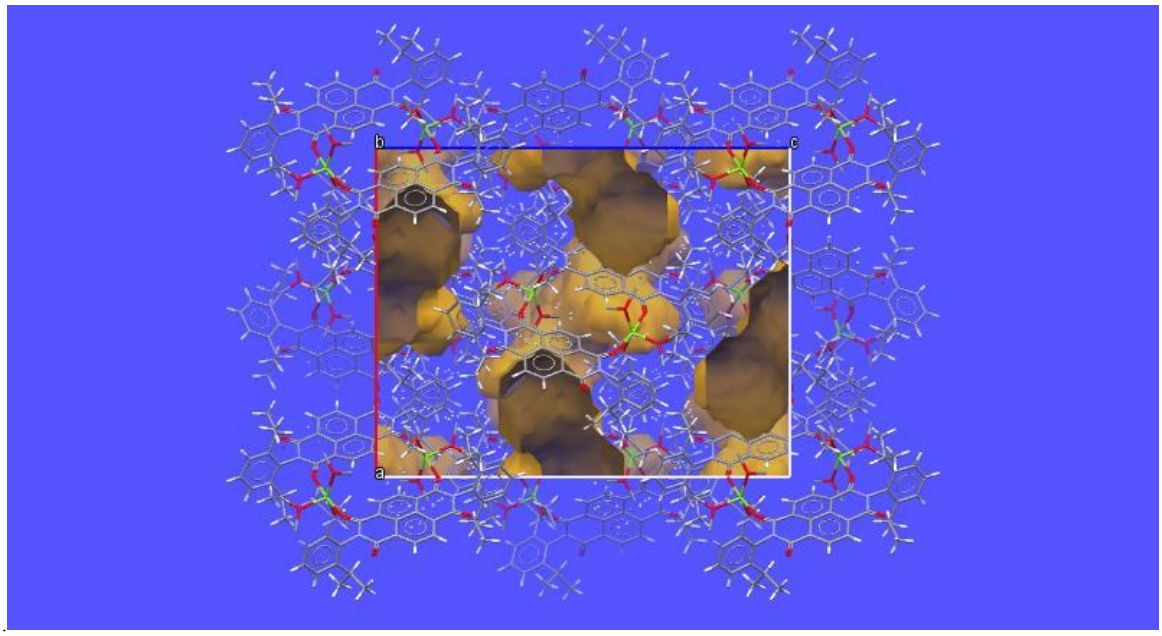

Figure S16. Cavity area in *bc* projection of solid state structure of **2.**

Table 2. XYZ coordinates of DFT optimized structure of *anti*-H_2[$Dipp_2$NDI].

Tag	Symbol	X	Y	Z
1	O	3.562876	0.000263	2.276262
2	C	2.855432	0.000147	1.263987
3	N	3.489506	-9E-06	-0.02284
4	C	4.94289	0.000002	-0.05018
5	C	5.619717	1.238974	-0.0535
6	C	7.02017	1.208076	-0.08712
7	C	7.71401	0.000042	-0.10646
8	C	7.020206	-1.20801	-0.08703
9	C	5.619755	-1.23895	-0.05339
10	C	4.886194	-2.57409	0.028369
11	C	5.095037	-3.21922	1.414961
12	C	5.287333	-3.53783	-1.10494
13	C	4.886113	2.574093	0.0282
14	C	5.287199	3.537784	-1.10517
15	C	5.094953	3.219306	1.414754
16	C	2.803412	-0.00015	-1.2075
17	O	3.506418	-0.00029	-2.35754
18	C	1.413163	-0.00016	-1.2513
19	C	0.719894	-7E-06	0.004917
20	C	1.411739	0.000137	1.230184
21	C	0.689557	0.000278	2.469179
22	C	-0.67296	0.000277	2.481929
23	C	-1.42326	0.000139	1.251525
24	C	-0.71974	-7E-06	-0.00409
25	C	-1.40547	-0.00015	-1.22876
26	C	-2.85539	-0.00014	-1.26287
27	O	-3.54707	-0.0003	-2.28289
28	N	-3.49673	-1E-06	0.016329
29	C	-2.81327	0.000134	1.197672
30	O	-3.61472	0.000264	2.288075
31	C	-4.95369	0.000001	0.023719
32	C	-5.62652	1.234955	0.016477
33	C	-4.89277	2.57189	-0.01666
34	C	-5.29046	3.480713	1.162698
35	C	-5.10259	3.282735	-1.36952
36	C	-7.02696	1.206678	0.012433
37	C	-7.72297	0.000009	0.012325
38	C	-7.02697	-1.20667	0.012617
39	C	-5.62653	-1.23495	0.016668
40	C	-4.89279	-2.5719	-0.01628
41	C	-5.10261	-3.28293	-1.36904
42	C	-5.2905	-3.48055	1.163201
43	C	-0.6862	-0.0003	-2.46912
44	C	0.677006	-0.00031	-2.48635
45	H	7.573942	2.141754	-0.08693
46	H	8.800061	0.000057	-0.12936
47	H	7.574006	-2.14167	-0.08677

48	H	3.814688	-2.38104	-0.07751
49	H	4.509368	-4.14192	1.493033
50	H	4.781577	-2.53898	2.211615
51	H	6.148494	-3.47502	1.576144
52	H	4.694088	-4.45624	-1.04209
53	H	5.11689	-3.09394	-2.09162
54	H	6.342859	-3.8236	-1.04175
55	H	3.814612	2.380999	-0.07764
56	H	4.693935	4.456188	-1.04235
57	H	5.116739	3.093839	-2.09182
58	H	6.342721	3.823584	-1.04202
59	H	4.509257	4.141997	1.492783
60	H	4.781523	2.539103	2.211451
61	H	6.148403	3.47515	1.575913
62	H	1.263819	0.00038	3.388504
63	H	-1.18136	0.000377	3.443969
64	H	-3.82079	2.374765	0.078662
65	H	-5.13052	2.978862	2.122511
66	H	-6.34451	3.774401	1.109289
67	H	-4.69179	4.398448	1.151431
68	H	-4.79064	2.641379	-2.19867
69	H	-6.15626	3.544651	-1.5189
70	H	-4.51838	4.209376	-1.40676
71	H	-7.57946	2.141515	0.002764
72	H	-8.80939	0.000012	0.006708
73	H	-7.57948	-2.1415	0.003086
74	H	-3.82081	-2.37477	0.079019
75	H	-4.79064	-2.64169	-2.19828
76	H	-6.15628	-3.54485	-1.51839
77	H	-4.51841	-4.20958	-1.40615
78	H	-5.13055	-2.97858	2.122947
79	H	-4.69185	-4.3983	1.152055
80	H	-6.34455	-3.77423	1.109833
81	H	1.223693	-0.00042	-3.42207
82	H	-1.26483	-0.00041	-3.38567
83	H	-3.07244	0.00039	3.088349
84	H	4.459731	-0.00027	-2.1603

Table 3. XYZ coordinates of DFT optimized structure of *syn*-H_2[$Dipp_2$NDI].

Tag	Symbol	X	Y	Z
1	O	-3.52203	-3.3E-05	2.356993
2	C	-2.80262	-2.2E-05	1.21137
3	N	-3.49642	-3E-06	0.014052
4	C	-4.94884	-3E-06	0.039289
5	C	-5.62715	-1.23856	0.041627
6	C	-7.02772	-1.20797	0.070987
7	C	-7.72174	-7E-06	0.087926
8	C	-7.02772	1.207961	0.071076
9	C	-5.62715	1.23855	0.041716
10	C	-4.89372	2.574097	-0.03408
11	C	-5.29229	3.530063	1.106802
12	C	-5.10566	3.229607	-1.41524
13	C	-4.89371	-2.5741	-0.03428
14	C	-5.10566	-3.22949	-1.41549
15	C	-5.29228	-3.53016	1.106523
16	C	-2.86123	0.000011	-1.25641
17	O	-3.54886	0.000036	-2.27775
18	C	-1.39999	0.000012	-1.22609
19	C	-0.71454	-8E-06	0.003734
20	C	-1.42656	-2.6E-05	1.257186
21	C	-0.68331	-4.5E-05	2.497507
22	C	0.673755	-4.6E-05	2.495286
23	C	1.430682	-2.9E-05	1.258938
24	C	0.714873	-0.00001	0.005015
25	C	1.400611	0.000008	-1.22278
26	C	2.864212	0	-1.25373
27	O	3.540406	0.000041	-2.28122
28	N	3.503209	-8E-06	0.012761
29	C	2.809656	-2.4E-05	1.202257
30	O	3.62394	-3.2E-05	2.286836
31	C	4.959494	0.000002	0.02338
32	C	5.633548	-1.23461	0.018228
33	C	4.900132	-2.57181	-0.01118
34	C	5.294816	-3.47471	1.173789
35	C	5.113785	-3.29009	-1.35947
36	C	7.034023	-1.20661	0.015358
37	C	7.730118	0.000023	0.015263
38	C	7.034005	1.206641	0.015407
39	C	5.63353	1.234627	0.018278
40	C	4.900091	2.571811	-0.01106
41	C	5.113734	3.290158	-1.35933
42	C	5.294759	3.47466	1.173942
43	C	0.689403	0.000032	-2.44874
44	C	-0.68678	0.000034	-2.45113
45	H	-7.58153	-2.14169	0.069311
46	H	-8.80789	-9E-06	0.10704
47	H	-7.58154	2.141677	0.069472

48	H	-3.82224	2.379528	0.068695
49	H	-4.70037	4.449677	1.048208
50	H	-5.11816	3.079337	2.089735
51	H	-6.34843	3.814806	1.048856
52	H	-4.51964	4.15245	-1.48836
53	H	-4.7947	2.556048	-2.21851
54	H	-6.15928	3.487161	-1.57234
55	H	-3.82223	-2.37953	0.068506
56	H	-4.51963	-4.15233	-1.48869
57	H	-4.79469	-2.55587	-2.21871
58	H	-6.15928	-3.48703	-1.57261
59	H	-4.70036	-4.44977	1.047847
60	H	-5.11814	-3.07952	2.089493
61	H	-6.34842	-3.81489	1.04856
62	H	-1.23263	-5.8E-05	3.431688
63	H	1.186679	-0.00006	3.45483
64	H	3.828074	-2.3738	0.080952
65	H	5.131901	-2.96778	2.130393
66	H	6.349155	-3.7682	1.124799
67	H	4.696474	-4.39273	1.165487
68	H	4.804463	-2.65398	-2.19369
69	H	6.167852	-3.55275	-1.50462
70	H	4.529782	-4.21697	-1.39358
71	H	7.586587	-2.14146	0.007039
72	H	8.816562	0.000032	0.01037
73	H	7.586555	2.141508	0.007129
74	H	3.828037	2.37378	0.081054
75	H	4.804423	2.654076	-2.19357
76	H	6.167796	3.552846	-1.50447
77	H	4.529714	4.217028	-1.3934
78	H	5.131856	2.967684	2.130522
79	H	4.696399	4.392668	1.165685
80	H	6.349092	3.768173	1.124964
81	H	-1.25398	0.000049	-3.37502
82	H	1.260201	0.000045	-3.37039
83	H	3.089103	-0.00004	3.091648
84	H	-4.47209	-2.7E-05	2.147872

References.

S1. M. J. M. Nesset, N. V. Shokhirev, P. D. Enemark, S. E. Jacobson and F. A. Walker, *Inorg. Chem.*, 1996, **35**, 5188-5200.

S2. Apex2, Version 2 User Manual, M86-E01078, Bruker Analytical X-ray Systems, Madison, WI, June 2006.

S3. A. Altomare, G. Cascarano, C. Giacovazzo, A. Guagliardi, M. C. Burla, G. Polidori and M. Camalli, *J. Appl. Crystallogr.*, 1994, **27**, 435-435.

S4. (a) P. W. Betteridge, J. R. Carruthers, R. I. Cooper, K. Prout and D. J. Watkin, *J. Appl. Cryst.*, 2003, **36**, 1487; (b) C. K. Prout and L. J. Pearce, CAMERON, Chemical Crystallography Laboratory, Oxford, UK, 1996.

S5. R. I. Cooper, A. L. Thompson and D. J. Watkin, *J. Appl. Cryst.*, 2010, **43**, 1100-1107.

S6. C. F. Macrae, I. J. Bruno, J. A. Chisholm, P. R. Edgington, P. McCabe, E. Pidcock, L. Rodriguez-Monge, R. Taylor, J. van de Streek and P. A. Wood, *J. Appl. Cryst.*, 2008, **41**, 466-470.

S7. (a) A. L. Spek, PLATON, A Multipurpose Crystallographic Tool, 1998; (b) A. L. Spek, *Acta Crystallogr. Sect. C*, 2015, **71**, 9-18; (c) P. van der Sluis and A. L. Spek, *Acta Cryst A*, 1990, **46**, 194-201.